

Radiation Shielding Studies Of $\text{Li}_2 \text{B}_4 \text{O}_7 - \text{TeO}_2 - \text{CuO}$ Glasses Modified With BaF_2

BSrikantha Chary^{1*}, B Srinivas², Md Shareefuddin¹

(Department Of Physics, Osmania University, Hyderabad, 500007, Telangana, India)

(Department Of Physics, VNR Vignan Jyothi Institute Of Engineering And Technology, Hyderabad-500090, Telangana, India)

Abstract:

This study presents an in-depth evaluation of gamma radiation shielding performance in a series of BLTC glass systems modified with varying levels of BaF_2 . Key radiation interaction parameters—including the linear attenuation coefficient, mass attenuation coefficient, half-value layer, mean free path, effective atomic number, effective electron density, and buildup factors—were systematically analyzed over a broad range of photon energies. The experimental results reveal that the attenuation properties follow an exponential decay, in agreement with the Beer–Lambert law, while exhibiting notable enhancements near the K-absorption edges of tellurium and barium. Comparative analyses indicate that a higher BaF_2 concentration, particularly in the BLTC-40 composition, significantly improves photon absorption capabilities, outperforming both conventional shielding glasses and concrete materials. These findings emphasize the importance of compositional optimization for developing advanced materials with superior radiation protection performance.

Key Word: Radiation shielding, attenuation coefficients, BaF_2 glasses, Tellurite glasses

Date of Submission: 28-02-2025

Date of Acceptance: 09-03-2025

I. Introduction

The continuous quest for effective radiation shielding materials has driven considerable research into glass systems doped with heavy metal oxides. Gamma rays, with their high energy and penetrating power, necessitate materials that can attenuate photon energy efficiently while maintaining desirable physical properties. In this context, the BLTC glass series—with its variable incorporation of BaF_2 —offers a promising pathway for tailoring shielding performance.

This work focuses on a comprehensive assessment of BLTC glasses by investigating key parameters such as the linear attenuation coefficient (μ), mass attenuation coefficient (μ/ρ), half-value layer (HVL), and mean free path (λ). The study further examines the effective atomic number (Z_{eff}) and effective electron density (N_{eff}) to understand how changes in chemical composition influence photon interactions at various energies. Additionally, buildup factors are evaluated to capture the complexity of secondary photon production under broad beam conditions. By correlating these parameters with the material composition, particularly the increasing presence of heavy elements like barium, the research aims to identify the optimal configuration for gamma radiation shielding applications [1-3].

II. Experimental

Before synthesizing the glass samples, an extensive review of compositional systems was conducted to identify materials with optimal radiation shielding potential. The selected glass series, formulated as $x\text{BaF}_2 - (89-x)\text{Li}_2 \text{B}_4 \text{O}_7 - 10\text{TeO}_2 - 1\text{CuO}$ (where $x = 0, 10, 20, 30,$ and 40 mol%), was designed to integrate high-density and radiation-attenuating components. The raw precursors—lithium tetraborate ($\text{Li}_2 \text{B}_4 \text{O}_7$), tellurium dioxide (TeO_2), barium fluoride (BaF_2), and copper oxide (CuO)—were procured from Sigma-Aldrich (purity >99%). Lithium borate was chosen for its neutron moderation properties, while TeO_2 and BaF_2 were prioritized for their high atomic number constituents to enhance photon absorption. CuO served as a stabilizer and modifier. The glasses were synthesized via a conventional melt-quenching technique. Precise stoichiometric quantities of each reagent were measured using a digital balance and homogenized by dry grinding in an agate mortar. The mixtures were melted in platinum crucibles at 1050°C for 1 hour in an electric furnace to ensure bubble-free homogeneity. The molten batches were rapidly quenched between preheated (100°C) stainless steel plates to form transparent glasses, followed by annealing at 100°C for 2 hours to minimize internal stress. The final compositions (labeled BFLBCu0–BFLBCu40) are detailed in Table 1.

To systematically evaluate radiation shielding performance, the Phy-X/PSD computational tool was employed across a broad energy spectrum (0.015–15 MeV). This software is widely recognized for its accuracy in modeling photon interactions with shielding materials. Key parameters—including the mass attenuation coefficient (MAC), linear attenuation coefficient (LAC), half-value layer (HVL), mean free path (MFP), and effective atomic number (Z_{eff})—were calculated to quantify shielding efficiency. These metrics provide critical insights into the glasses' ability to attenuate gamma rays, with lower HVL and MFP values indicating superior shielding capacity. The progressive substitution of $\text{Li}_2\text{B}_4\text{O}_7$ with BaF_2 aimed to enhance density and high-Z Ba content, directly correlating with improved photon absorption.

Glass code	BaF_2	$\text{Li}_2\text{B}_4\text{O}_7$	TeO_2	CuO
BLTC-0	0	89	10	1
BLTC-10	10	79	10	1
BLTC-20	20	69	10	1
BLTC-30	30	59	10	1
BLTC-40	40	49	10	1

Table 1 Glass composition in mole % with glass code

III. Results And Discussions

LAC and MAC

The primary parameters evaluated were the linear attenuation coefficient (μ) and the mass attenuation coefficient (μ/ρ), which measure the material's capacity to attenuate photon energy. The attenuation trends, presented in Fig.1, demonstrate an overall decrease in both μ and μ/ρ values, following an exponential decay in line with the Beer-Lambert law:

$$I = I_0 e^{-\mu t} \quad (1)$$

where I_0 and I represent the initial and reduced photon intensities, respectively, μ is the linear attenuation coefficient, and t denotes the material thickness.

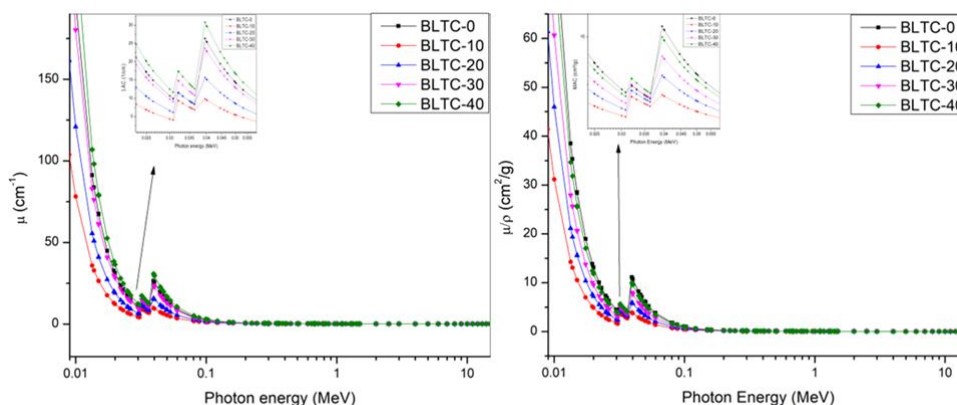


Figure 1. Variation of LAC and MAC with photon energy.

The values of μ and μ/ρ continue to decrease consistently until a notable increase is observed around ~30 keV and ~40 keV. These increases can be linked to the photoelectric absorption (PA) effect, which is particularly pronounced near the K-absorption edges of Tellurium (approximately 31.8 keV) and Barium (around 37.4 keV). The rise in attenuation coefficients at these energies arises from the heightened probability of photon interactions with K-electrons in Tellurium and Barium atoms. This pattern aligns with theoretical predictions, which suggest that elements with higher atomic numbers exhibit significant photoelectric effects near their absorption edges. Beyond 40 keV, the attenuation coefficients decline, indicating a shift where Compton scattering (CS) becomes more prevalent than PA. This reduction is consistent with the inverse relationship between the PA cross-section and photon energy, typically characterized by an exponent between 3 and 5.[4-9]

Half-Value Layer (HVL) and Mean Free Path (MFP)

The half-value layer (HVL), denoted as $d_{1/2}$, is a critical parameter in assessing the shielding efficacy of materials against photon radiation. It represents the thickness required to reduce the intensity of an incident photon beam by 50%. Mathematically, $d_{1/2}$ is inversely related to the linear attenuation coefficient (AC), as shown in Equation (2):

$$d_{1/2} = \frac{\ln 2}{\mu} = \frac{\ln 2}{(\rho \times (\mu/\rho))} \quad (2)$$

where μ is the linear attenuation coefficient, ρ is the material density, and μ/ρ is the mass attenuation coefficient. As photon energy increases, $d_{1/2}$ rises due to the reduced interaction cross-section of higher-energy photons with matter. This relationship is evident in the results for BLTC glasses.

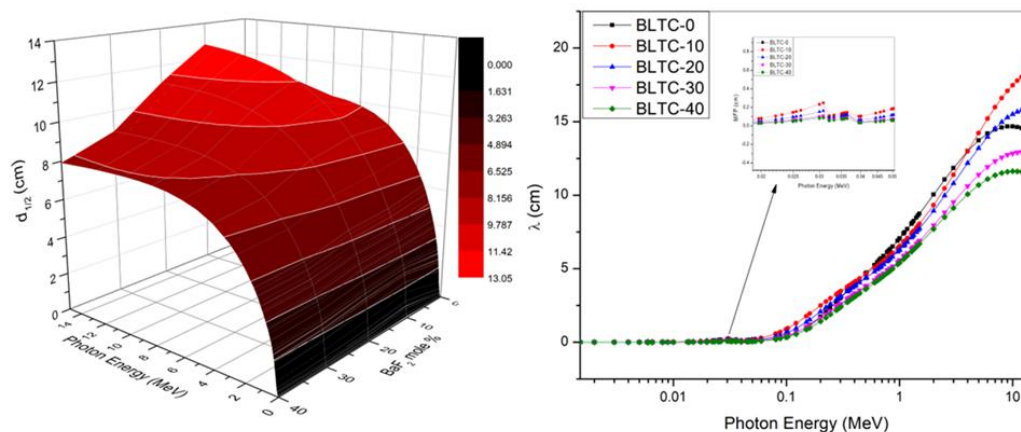


Figure 2. Variation of HVL and MFP with photon energy.

As we can see from **Fig.2**, HVL values are increased from BLTC-0 to BLTC-10 as we introduced BaF_2 into the glass matrix, and from BLTC-10 to BLTC-40 it decreases at every energy level. This may be due to the increase in BO_3 units as we introduced Barium into the glass matrix. The rise in BO_3 units facilitates the photons to pass through the material more easily, and a further increment of the BaF_2 content significantly influences photon absorption due to its high atomic number, which enhances interaction probabilities. These trends illustrate a clear dependency of $d_{1/2}$ on glass composition. Among the samples, BLTC-40 exhibited the lowest $d_{1/2}$, establishing it as the most effective gamma radiation shield.

The mean free path (λ) is another crucial parameter that describes the average distance photons travel between successive interactions in a material. A shorter λ indicates greater photon interaction and better shielding performance. The relationship between λ and μ is given as:

$$\lambda = 1/\mu \quad (3)$$

For the BLTC glasses, λ ranges from $\sim 70 \mu\text{m}$ to 18.5 cm as photon energy increases. The trend reflects the increased interaction of higher-energy photons with the increment in the BaF_2 content in the glasses. Comparative analyses reveal the superior shielding performance of BLTC-40. For instance, between the photon energies of $\sim 0.5 \text{ MeV}$, and $\sim 5 \text{ MeV}$, BLTC-0 exhibited higher λ values than the remaining glasses in the series, this may be due to the absence of heavy metal ion (Ba) as Compton scattering is the dominant mechanism of radiation protection in this energy range. Compared to radiation shielding glasses like RS 253, RS 253 G18, RS 253 G19, and RS 360 [5]. Similarly, in comparisons with high photon-absorbing glasses (e.g., PBZH3, PBCN-M4, S8, ZBP4, and BSNW4), the λ values of BLTC -40 were consistently lower across a wide energy spectrum (15 keV–15 MeV). Further comparisons with shielding concrete such as ordinary concrete, hematite-serpentine, ilmenite-limonite, basalt-magnetite, steel-scrap, and steel-magnetite also demonstrated the superiority of BLTC -40, as its λ values remained lower throughout the energy range. Notably, the increased addition of BaF_2 improved the photon absorption properties of glasses, reducing $d_{1/2}$ and λ . These trends underscore the importance of optimizing glass composition to enhance shielding performance, particularly for high-energy photon applications [10-12].

Z_{eff} and N_{eff}

The effective atomic number (Z_{eff}) and effective electron density (N_{eff}) are essential parameters for understanding the interaction of gamma radiation with composite materials such as BLTC glass systems. These parameters shown in **Fig.3** provide critical insights into radiation shielding efficiency, photon absorption, and dosimetric applications. Z_{eff} is a measure of the overall atomic number of a composite material, accounting for contributions from its constituent elements. It is calculated using mass attenuation coefficients (μ/ρ) and weight fractions of the elements present in the material. The Z_{eff} values for BLTC glasses exhibit variations across different photon energies, following the general trend observed in other glass compositions used for radiation shielding. The decline in Z_{eff} values is prominent within the 0.4–2 MeV range due to the dominance of Compton scattering (CS), which is less dependent on the chemical composition. Beyond this range, Z_{eff} increases as the photoelectric (PE) and pair production (PP) interactions become more significant at lower and higher energies,

respectively. If we observe throughout the glass series BLTC-0 has the highest Z_{eff} at all energy levels, which may be due to a higher refractive index, which suggests greater electronic polarizability, which can enhance the probability of photon interactions within the material. Higher Z_{eff} values correspond to improved photon attenuation capabilities. In BLTC glasses, variations in Z_{eff} depend on the specific elemental composition, apart from BLTC-0, with higher atomic weight elements increasing Z_{eff} , and thereby improving the gamma shielding performance[13-16].

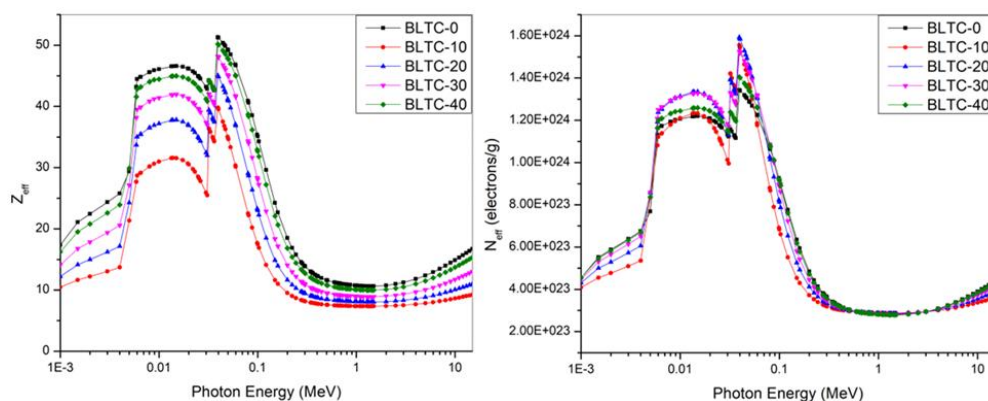


Figure 3. Variation of Z_{eff} and N_{eff} with photon energy.

N_{eff} represents the number of electrons per unit mass available for photon interactions. It is directly related to Z_{eff} and inversely proportional to average molecular weight. The relationship between N_{eff} and photon energy shows a decline within the 0.4–2 MeV energy range due to the reduced influence of chemical composition in CS interactions. At lower and higher photon energies, N_{eff} increases, reflecting the enhanced contribution of PE and PP interactions, respectively. The N_{eff} values in BLTC glasses exhibit fluctuations across different compositions, with materials containing higher atomic number elements demonstrating greater electron densities. This results in more efficient photon absorption and improved radiation shielding properties[17-18].

Buildup factors

In radiation shielding applications, the accurate estimation of photon transmission characteristics is essential, particularly in broad beam conditions where secondary photon buildup becomes significant. The exposure buildup factor (EBF) and the energy-absorption buildup factor (EABF) are crucial parameters in evaluating the shielding efficiency of any glass system. Under broad beam transmission conditions, incident photons undergo multiple interactions within the glass, leading to the production of secondary photons. This results in an increase in the photon transmission coefficient, thereby influencing the overall shielding performance. The buildup factors for BLTC glasses, considering various thicknesses up to 40 mean free paths (mfp) shown in **Fig. 4**. The results indicate that both EBF and EABF exhibit dependencies on photon energy, penetration depth, and glass composition.

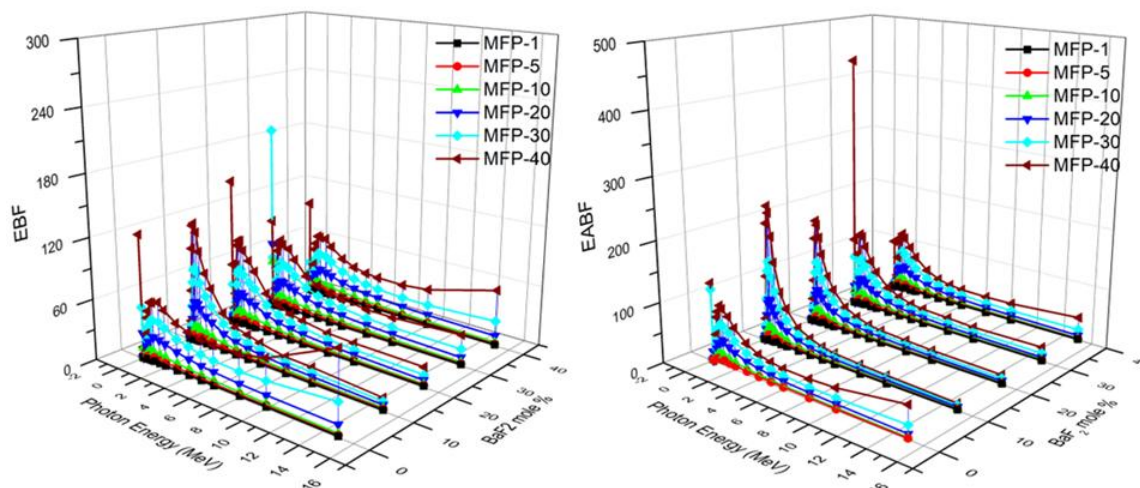


Figure 1, Variation of EBF and EABF at different MFPs with photon energy.

At lower photon energies, particularly around 30 keV, and 60 keV, a high buildup factor is observed, which can be attributed to the strong photoelectric absorption by elements such as Ba and Te. This absorption leads to subsequent de-excitation processes, contributing to increased photon interactions within thicker glass samples. As photon energy increases, Compton scattering becomes the dominant interaction mechanism, leading to further increases in EBF and EABF values. This effect is particularly pronounced at intermediate photon energies, around 0.8 MeV, where the probability of Compton scattering is at its peak. For BLTC glasses with varying compositions, the presence of heavy element such as Ba plays a significant role in influencing the buildup factors. The increase in EBF and EABF with BaF_2 content suggests enhanced photon interaction probabilities, thereby contributing to greater photon retention within the shielding material. Additionally, at higher photon energies, secondary photon production through processes such as electron-positron annihilation further amplifies the buildup effect, especially at greater depths. Comparative analysis of EBF across different photon energy levels reveals that at lower energies (0.015–0.15 MeV), the values remain relatively low, with EBF approaching unity for specific glass compositions and depths. This behavior suggests that narrow beam transmission conditions are sufficient at these energy levels. However, as photon energy increases beyond 1.5 MeV, the buildup factor becomes more dependent on the effective atomic number (Z_{eff}) of the glass, with Compton scattering playing a dominant role [19–20].

Overall, the analysis of EBF and EABF for BLTC glass systems highlights the importance of glass composition and thickness in determining shielding effectiveness. The findings underscore the necessity of accounting for photon buildup effects in practical radiation shielding applications, ensuring accurate dosimetric assessments and optimized material design.

IV. Conclusions

The systematic investigation of the BLTC glass systems has revealed significant insights into their gamma radiation shielding capabilities. The analysis confirmed that the attenuation of photon energy in these materials adheres to the exponential decay described by the Beer–Lambert law, with marked deviations near the K-absorption edges of tellurium and barium due to enhanced photoelectric absorption. Findings from the half-value layer and mean free path assessments indicate that an increased BaF_2 content, especially in the BLTC-40 composition, leads to superior photon attenuation performance. The study also demonstrates that both the effective atomic number and electron density are strongly influenced by the material's composition, thereby affecting the interaction probabilities for incoming photons. Moreover, the buildup factor evaluations underscore the importance of considering secondary photon effects, particularly at intermediate energies where Compton scattering predominates. Overall, the optimized BLTC glass compositions, notably those enriched with BaF_2 , emerge as highly effective candidates for gamma radiation shielding. Future work should extend these findings by exploring further compositional variations and practical considerations to advance the development of robust, multifunctional shielding materials for high-energy photon applications.

References

- [1]. Nagaraju G, Alharshan GA, Chandra Sekhar K, Alrowaili ZA, Shareefuddin M, Olarinoye IO, Et Al. Significant Impact Of Lead(II) Chloride On Synthesis And Properties Of Boron-Based Metallic Glasses For Mechanical, Optical, And Radiation Applications. *Journal Of Materials Science: Materials In Electronics* 2023;34. <https://doi.org/10.1007/S10854-022-09742-0>.

- [2]. Singh RU, Sekhar KC, Alzahrani JS, Alrowaili ZA, Shareefuddin M, Purushotham Y, Et Al. Effect Of Moo_3 On $Na_2O-B_2O_3-CdO-ZnO$ Glasses: Applications In Optoelectronics, Communication Devices, And Radiation Shielding. *Ceram Int* 2023;49:11600–11. <https://doi.org/10.1016/j.ceramint.2022.12.007>.
- [3]. Sekhar KC, Hameed A, Narsimlu N, Alzahrani JS, Alothman MA, Olariyoie IO, Et Al. Synthesis, Optical, Structural, And Radiation Transmission Properties Of $PbO/Bi_2O_3/B_2O_3/Fe_2O_3$ Glasses: An Experimental And In Silico Study. *Opt Mater (Amst)* 2021;117. <https://doi.org/10.1016/j.optmat.2021.111173>.
- [4]. Olariyoie, O., 2020. Computational Methods In Nuclear Radiation Shielding And Dosimetry: AMBIENT DOSE BUILDUP FACTORS. NOVA Science Publisher.
- [5]. Olariyoie, O., Mohammed, B., 2019. Photon Absorption Buildup Factors For Different Concrete Types. *African J. Med. Phys.* 2 (1), 31–37, 2019.
- [6]. Knoll, G.F., 2010. Radiation Detection And Measurement, Third Ed. John Wiley & Sons, Inc, New York, Chichester, Weinheim, Brisbane, Toronto, Singapore.
- [7]. Samdani M, Basha B, Alsufyani SJ, Kebaili I, Sekhar KC, Alrowaili ZA, Et Al. Gamma Shielding Performance Of B_2O_3/BaO -Based Glassy System: Synthesis And Simulation Study. *Radiation Physics And Chemistry* 2024;214. <https://doi.org/10.1016/j.radphyschem.2023.111301>.
- [8]. Olariyoie, I.O., Alomairy, S., Sriwunkum, C., Al-Buriah, M.S., 2021. Effect Of Ag_2O/V_2O_5 Substitution On The Radiation Shielding Ability Of Tellurite Glass System Via XCOM Approach And FLUKA Simulations. *Phys. Scripta* 96 (6), 065308.
- [9]. Rammah, Y.S., Al-Buriah, M.S., Abouhaswa, A.S., 2020. $B_2O_3-BaCO_3-Li_2O_3$ Glass System Doped With Co_3O_4 : Structure, Optical, And Radiation Shielding Properties. *Phys. B Condens. Matter* 576, 411717. <https://www.schott.com/en-ca/products/radiation-shielding-glasses/productvariants?Tab=Rs-Glass-Series>.
- [10]. P. Kaur, K.J. Singh, S. Thakur, P. Singh, B.S. Bajwa, Investigation Of Bismuth Borate Glass System Modified With Barium For Structural And Gamma-Ray Shielding Properties, *Spectrochim. Acta Part A Mol. Biomol. Spectrosc.* 206 (2019) 367–377, <https://doi.org/10.1016/j.saa.2018.08.038>.
- [11]. I.I. Bashter, Calculation Of Radiation Attenuation Coefficients For Shielding Concretes, *Ann. Nucl. Energy* 24 (17) (1997) 1389–1401 1997, [https://doi.org/10.1016/S0306-4549\(97\)00003-0](https://doi.org/10.1016/S0306-4549(97)00003-0).
- [12]. M.S. Alburiah, H.H. Hegazy, F. Alresheedi, I.O. Olariyoie, H. Algarni, H.O. Tekin, Effect Of CdO Addition On Photon, Electron, And Neutron Attenuation Properties Of Boro-Tellurite Glasses. *Ceram. Int.* (2020). <https://doi.org/10.1016/j.ceramint.2020.10.168>
- [13]. Y.S. Rammah, H.O. Tekin, C. Sriwunkum, I. Olariyoie, A. Alalawi, M.S. Al-Buriah, T. Nutaro, B.T. Tonguc, Investigations On Borate Glasses Within SBC-Bx System For Gamma-Ray Shielding Applications. *Nucl. Eng. Tech.* 53(1), 282–293 (2021). <https://doi.org/10.1016/j.net.2020.06.034>
- [14]. Al-Buriah, M.S., Hegazy, H.H., Alresheedi, F. Et Al. Effect Of Sb_2O_3 Addition On Radiation Attenuation Properties Of Tellurite Glasses Containing V_2O_5 And Nb_2O_5 . *Appl. Phys. A* 127, 106 (2021). <https://doi.org/10.1007/S00339-020-04265-Z>
- [15]. I.O. Olariyoie, F.I. El-Agawany, A. El-Adawy, E.S. Yousef, Y.S. Rammah, Mechanical Features, Alpha Particles, Photon, Proton, And Neutron Interaction Parameters Of $TeO_2-V_2O_5-Moo_3$ Semiconductor Glasses. *Ceram. Int.* 46(14), 23134–23144 (2020). <https://doi.org/10.1016/j.ceramint.2020.06.093>
- [16]. G.J. Hine, The Effective Atomic Numbers Of Materials For Various Gamma Ray Interactions. *Phys. Rev.* 85, 725 (1952)
- [17]. Olariyoie, I.O. (2011). Variation Of Effective Atomic Numbers Of Some Thermoluminescence And Phantom Materials With Photon Energies. *Res. J. Chem. Sci.* 1(2): 64–69. <http://www.isca.in/>.
- [18]. I.O. Olariyoie, R.I. Odiaga, Silas Paul, Exabcal: A Program For Calculating Photon Exposure And Energy Absorption Buildup Factors, *Heliyon* 5 (7) (2019), E02017.
- [19]. Singh, V.P., Badiger, N.M., Kaewkhao, J., 2014. Radiation Shielding Competence Of Silicate And Borate Heavy Metal Oxide Glasses: Comparative Study. *J. Non-Cryst. Solids* 404, 167–173.